

Power-Aware Distributed Target Detection in Wireless Sensor Networks with UWB-Radar Nodes

Daniel Bielefeld, Rudolf Mathar
Institute for Theoretical Information Technology
RWTH Aachen University
D-52056 Aachen, Germany
{bielefeld, mathar}@ti.rwth-aachen.de

Ole Hirsch, Reiner S. Thomä
Electronic Measurement Research Lab
Ilmenau University of Technology
D-98684 Ilmenau, Germany
{ole.hirsch, reiner.thomae}@tu-ilmenau.de

Abstract—Distributed detection of targets is one of the major applications of wireless sensor networks. Many existing results on distributed detection are either derived from analytical models or are based on simulations. In this paper, the performance of a distributed target detection system is evaluated by real measurement data obtained by UWB-radar-based sensor nodes. After local processing of the radar signal, the sensor nodes transmit their local decisions about the absence or presence of the target to a fusion center. For this purpose, a power-aware algorithm for resource allocation, which is tailored for UWB communication links is discussed. The feasibility and the effectiveness of this algorithm is evaluated by a hybrid approach based on the measurement data and simulations.

I. INTRODUCTION

The detection of targets in a region of interest is an important application of wireless sensor networks [1], [2]. In distributed detection, the sensor nodes process their observations locally and make preliminary decisions about the absence or presence of the target and transmit them to a fusion center for decision combining. As the communication channels between the sensor nodes and the fusion center are subject to noise and interference, it becomes necessary to take wireless channel conditions into account in order to optimally design the distributed detection system [3]. The channel quality can, e.g., be controlled by an appropriate assignment of transmission power levels.

One possible sensing technology for distributed detection applications is radar. Actually, the origin of the research on distributed detection was based on the attempt to fuse signals of different radar devices [4]. Currently, distributed detection is usually discussed in the context of wireless sensor networks, where the sensor unit of the nodes might be based on radar technology [5]. In the literature, many of the existing results on distributed detection are either derived analytically from a mathematical model or are based on simulations. The issue with these two approaches is that they might be based on simplifying assumptions to allow for analytical tractability or computational feasibility, respectively. Especially for radar-based sensors the measured observations might be considerably different from the commonly assumed constant signal in Gaussian noise model.

In this paper, we evaluate the performance of a distributed detection system with radar-based sensor nodes using real

radar measurement data. We use an ultra-wideband (UWB) M -sequence radar system [6] to detect three different target objects in a number of different scenarios in a distributed manner. Moreover, we propose to use impulse radio ultra-wideband (IR-UWB) [7] to transmit the local detection results to the fusion center. This enables sensor nodes completely based on UWB technology, which has low energy consumption and might be efficiently implemented in hardware - two major requirements of wireless sensor networks. To obtain high detection performance of the system in case of strictly limited energy resources, we discuss an application-specific strategy for the assignment of transmission power levels to the communication units. The approach aims to optimally distribute a given budget of total transmission power in terms of the global probability of detection error. The feasibility and the performance of the algorithm is evaluated using the measurement data combined with simulation data. The results show, that the approach leads to significant performance gains compared to uniform power assignment to the communication units.

The remainder of the paper is organized as follows. In Section II, distributed detection with noisy communication channels and in Section III the considered IR-UWB transmission scheme and the power assignment strategy are shortly introduced. The measurement setup is described in Section IV and Section V presents the processing of the measurement data. Numerical results of the global detection performance are given in Section VI and finally, in Section VII conclusions are drawn.

II. DISTRIBUTED DETECTION

The problem of distributed target detection in the parallel fusion network with noisy channels can be stated as follows (see Fig. 1). We consider a binary hypothesis testing problem with hypotheses H_0 and H_1 indicating the absence and presence of the target. The associated prior probabilities are $\pi_0 = P(H_0)$ and $\pi_1 = P(H_1)$. In order to detect the true state of nature, the network of sensors S_1, \dots, S_N collects an array of random observations $(X_1, \dots, X_N)' \in \mathcal{X}_1 \times \dots \times \mathcal{X}_N$. The random observations X_1, \dots, X_N are assumed to be conditionally independent across sensors given the underlying hypothesis and distributed according to $f_{X_j}(\cdot|H_0)$ and $f_{X_j}(\cdot|H_1)$ respec-

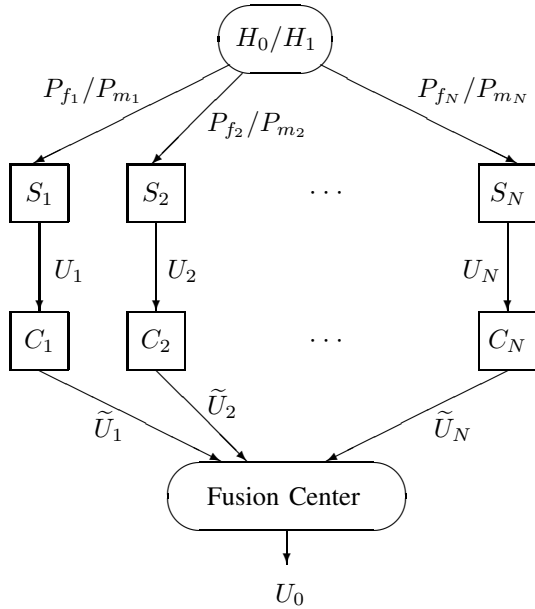


Fig. 1. Parallel fusion network with noisy channels.

tively. The nodes process their observations independently by forming local decisions

$$U_j = \delta_j(X_j), \quad j = 1, \dots, N. \quad (1)$$

In case of binary quantization, the node decision rules are mappings $\delta_j: \mathcal{X}_j \rightarrow \{0, 1\}$. Sensor decision rules leading to optimal configurations are monotone log-likelihood ratio (LLR) quantizers provided that the observations are conditionally independent across sensors [8]. Thus, we consider decision rules δ_j that can be parameterized by real-valued quantization thresholds θ_j . In this way, each local decision U_j is characterized by the following local false alarm and miss probabilities

$$P_{f_j} = P(U_j = 1|H_0) = P(L_j > \theta_j|H_0), \quad (2)$$

$$P_{m_j} = P(U_j = 0|H_1) = P(L_j \leq \theta_j|H_1), \quad (3)$$

where L_j is the local log-likelihood ratio of observation X_j . Upon local detection, the sensor nodes transmit the preliminary decisions U_1, \dots, U_N to the fusion center in order to perform decision combining. The communication channels C_1, \dots, C_N between the wireless sensors and the fusion center are usually subject to noise and interference. We model the communication link C_j between sensor S_j and the fusion center by a binary symmetric channel with bit-error probability ε_j , i.e.

$$\varepsilon_j = P(\tilde{U}_j = 1|U_j = 0) = P(\tilde{U}_j = 0|U_j = 1) \quad (4)$$

for $j = 1, \dots, N$. The potentially corrupted received detection results $\tilde{U}_1, \dots, \tilde{U}_N$ are combined to yield the final decision $U_0 \in \{0, 1\}$. As performance metric we consider the global probability of error

$$P_e = \pi_0 P_f + \pi_1 P_m \quad (5)$$

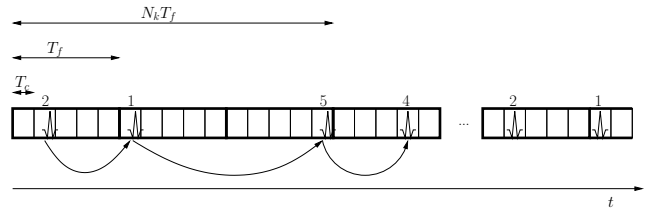


Fig. 2. Illustration of some IR-UWB parameters. In the example $c^{(k)} = (2, 1, 5, 4)$, $d_1^{(k)} = 1$, $d_2^{(k)} = 0$, and $N_k = 3$.

which can be written as a weighted sum of the global probability of false alarm $P_f = P(U_0 = 1|H_0)$ and the corresponding global probability of miss $P_m = P(U_0 = 0|H_1)$.

A. Optimal channel-aware fusion rule

Under the assumption of conditionally independent local detection results U_1, \dots, U_N and independent binary symmetric channels C_1, \dots, C_N , the optimal channel-aware fusion rule can be implemented by a linear threshold rule

$$\sum_{j=1}^N \tilde{\lambda}_j \tilde{U}_j \begin{cases} U_0 = 1 & \text{if} \\ \geq \vartheta & \\ U_0 = 0 & \text{otherwise} \end{cases} \quad (6)$$

with effective sensor weights

$$\tilde{\lambda}_j = \log \left(\frac{(1 - \tilde{P}_{f_j})(1 - \tilde{P}_{m_j})}{\tilde{P}_{f_j} \tilde{P}_{m_j}} \right) \quad (7)$$

for $j = 1, \dots, N$, and a decision threshold

$$\vartheta = \log \left(\frac{\pi_0}{\pi_1} \prod_{j=1}^N \frac{1 - \tilde{P}_{f_j}}{\tilde{P}_{m_j}} \right). \quad (8)$$

The modified error probabilities $\tilde{P}_{f_j} = P(\tilde{U}_j = 1|H_0)$ and $\tilde{P}_{m_j} = P(\tilde{U}_j = 0|H_1)$ can be calculated as

$$\begin{aligned} \tilde{P}_{f_j} &= P_{f_j} + \varepsilon_j(1 - 2P_{f_j}), \\ \tilde{P}_{m_j} &= P_{m_j} + \varepsilon_j(1 - 2P_{m_j}). \end{aligned} \quad (9)$$

III. TRANSMISSION OF LOCAL DECISIONS

A. Impulse Radio Ultra-Wideband

For transmitting the local decisions from the nodes to the fusion center, we consider impulse radio ultra-wideband (IR-UWB) with pulse position modulation with modulation index δ and pseudo random time hopping codes as multiple access scheme. The transmitted signal from sensor S_j to the fusion center can be written as

$$s_j(t) = A_j \sum_{i=-\infty}^{\infty} w(t - iT_f - c_i^{(j)}T_c - \delta d_{\lfloor i/N_j \rfloor}^{(j)}), \quad (10)$$

where T_f denotes the length of a time frame in which one impulse of form $w(t)$ is transmitted. The impulse is delayed by an integer multiple of the chip length T_c according to the time hopping code $c_i^{(j)}$. Each data bit $d_i^{(j)}$ corresponding to the

local decision U_j from (1) is transmitted by a number of N_j equally modulated pulses with amplitude A_j . If the transmitted signal of other nodes $S_{k \neq j}$ is treated as noise, the signal-to-interference and noise ratio (SINR) γ_j of the link between sensor S_j and the fusion center reads as

$$\gamma_j = N_j \frac{g_j p_j}{\sigma^2 \sum_{k \neq j} g_k p_k + \frac{1}{T_f} \eta}, \quad (11)$$

with p_j denoting the transmission power of sensor node S_j and σ^2 is a spreading gain parameter depending on the correlation properties of the employed pulse form. The path gain between sensor S_j and the fusion center is denoted by g_j . The energy of the additional noise is given by η . Some exemplary parameters for one node are illustrated in Fig. 2. More details can be found in [9].

B. Power assignment based on marginal analysis

The assignment of transmission power levels to the nodes should be performed in an application-specific way, with the goal to optimally distribute a given budget of total transmission power

$$p_{\text{tot}} = \sum_{j=1}^N p_j \quad (12)$$

with respect to the global probability of detection error P_e according to (5). We use the assignment strategy described in [10]. It is based on a marginal analysis of the effective sensor weight $\tilde{\lambda}$ given in (7). In this strategy the target SINR γ_j of the link between S_j and the fusion center is determined according to

$$\gamma_j = \left(\frac{g_j}{g_{\min}} \right) \cdot \left(\frac{\partial \tilde{\lambda}_j}{\partial \gamma_j} \right)^{-1}(\varrho), \quad (13)$$

where g_j is the path gain between S_j and the fusion center and g_{\min} is the minimum path gain of a node to the fusion center. Trade-off parameter ϱ can be used to balance total transmission power and the global detection quality. Using the standard Gaussian approximation as discussed in [11], the channel bit-error rate ε_j of node S_j can be stated as

$$\varepsilon_j = \frac{1}{2} \operatorname{erfc}(\sqrt{\gamma_j}). \quad (14)$$

It is equivalent to the bit-error probability of the binary symmetric channel C_j according to (4). The SINR γ_j from (13) can be realized by setting the transmission power of S_j to

$$p_j = \frac{\frac{\eta}{T_f \sigma^2}}{g_j \left(\frac{N_j}{\sigma^2 \gamma_j} + 1 \right) \left(1 - \sum_k \frac{1}{\frac{N_k}{\sigma^2 \gamma_k} + 1} \right)}. \quad (15)$$

Additional information to the approach is given in [10].



Fig. 3. Photograph of the measurement setup.

IV. PRACTICAL RADAR MEASUREMENTS

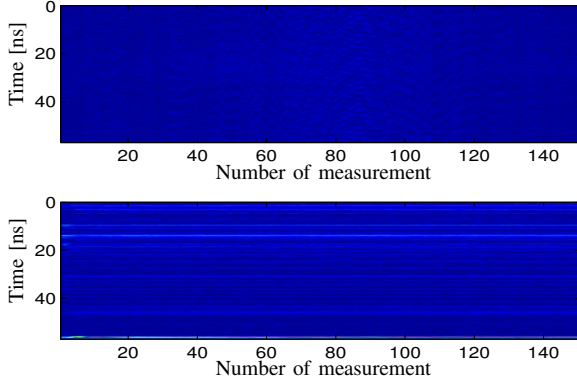
To validate the proposed concepts in practice, we conducted measurements using an UWB M -sequence radar [6]. The radar device is equipped with one transmit and four receive channels. While the transmitter employs a horn antenna, the four receivers use omnidirectional antennas.

For the measurements which were conducted indoors in a staircase, the transmitter and the receivers were placed on static positions around the static target object, which was mounted on the top of a polystyrene pillar. The four receivers sent their observations of the transmitter's radar signal via cables to the main radar unit which was connected to a computer, where the observations were stored for further processing. A photograph of the complete measurement setup is given in Fig. 3. We used three different target objects. A metal stick as shown in Fig. 3, which might behave as an omnidirectional point-scatterer of the radar signal, a metal box with a strongly directional reflection characteristic and finally a non-moving person.

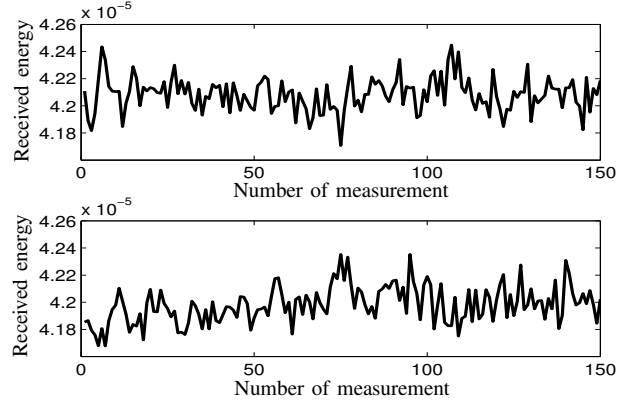
To generate different measurement scenarios, different configurations of attenuation elements attached to the cables were used. This allows for an independent control of the individually received signal strength and thus of the detection quality of the four receivers. For each target object and also with no object present, we took 150 measurements for each of the 10 different attenuation scenarios. The processing of the received and stored observations was done off-line.

V. PROCESSING OF MEASUREMENT DATA

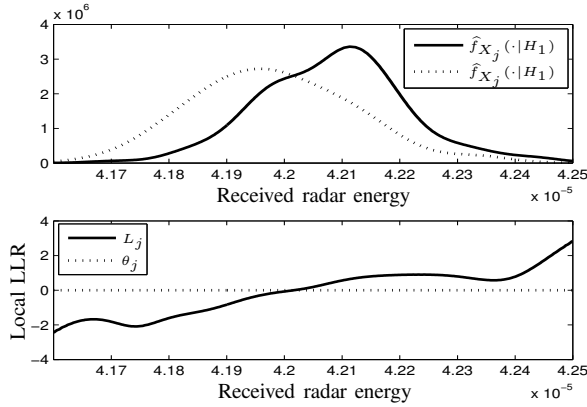
After some standard pre-processing like cross-correlation of the received signals with the transmitted M -sequence, the radargram for each node is achieved. In Fig. 4 a) typical radargrams of one sensor with absence (top) and presence (bottom) of the target object are shown. The received energy for each of the 150 measurements is obtained by integrating the square of the received signal. It is shown for the same measurement points in the lower part of Fig. 4 b). In the model from Section II the received energy of the nodes is modelled



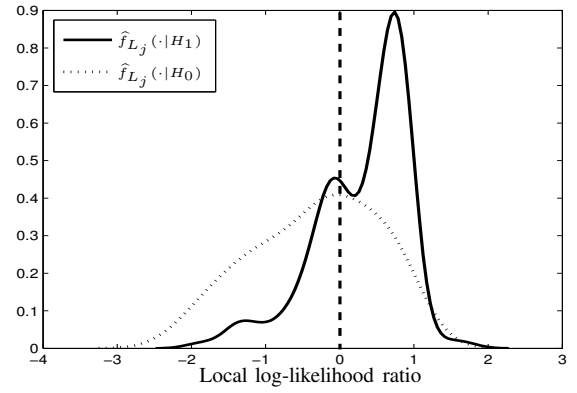
a) Radargram with absent (top) and present target object (bottom).



b) Received radar energy with absent (top) and present target object (bottom).



c) Estimated pdfs of the received energy (top) and the corresponding LLR (bottom)



d) Estimated pdfs of the local log-likelihood ratio.

Fig. 4. Illustration of the steps for the processing of the measurement data for an exemplary node

by X_1, \dots, X_N . To estimate the probability density functions (pdf) of the observations given the two hypothesis $f_{X_j}(\cdot|H_0)$ and $f_{X_j}(\cdot|H_1)$, we use a training sequence in which for every observation it is known whether the target object was present or not. These training sequences were used in a non parametric density estimation approach based on kernel smoothing [12] to obtain the estimates $\hat{f}_{X_j}(\cdot|H_0)$ and $\hat{f}_{X_j}(\cdot|H_1)$ of the pdfs. The upper picture in Fig. 4 c) shows the estimated pdfs for the same scenario as in Fig. 4 a) and Fig. 4 b). In practice, this initialization could, e.g., be performed in a training phase after the system has been deployed.

Locally optimal decision rules are obtained by quantizing the local log-likelihood ratio of the two pdfs as illustrated in the lower picture of Fig. 4 c). In case of binary decisions, decision threshold θ_j is equal to zero. Hence, sensor node S_j 's local decision u_j for the observation x_j is given by

$$\frac{\hat{f}_{X_j}(x_j|H_1)}{\hat{f}_{X_j}(x_j|H_0)} \begin{cases} u_j = 1 \\ \geq \\ u_j = 0 \end{cases} (\theta_j = 0). \quad (16)$$

The local error probabilities P_{f_j} and P_{m_j} can be locally estimated by using estimates of the conditional pdfs of the

LLR $f_{L_j}(\cdot|H_0)$ and $f_{L_j}(\cdot|H_1)$ as illustrated in Fig. 4 d). With the non-parametric estimates $\hat{f}_{L_j}(\cdot|H_0)$ and $\hat{f}_{L_j}(\cdot|H_1)$ of the pdfs, the local error probabilities are estimated by

$$\begin{aligned} \hat{P}_{f_j} &= \int_{\theta}^{\infty} \hat{f}_{L_j}(l|H_0)dl, \\ \hat{P}_{m_j} &= \int_{-\infty}^{\theta} \hat{f}_{L_j}(l|H_1)dl. \end{aligned} \quad (17)$$

The obtained estimates are then transmitted to the fusion center, where they are initially used to determine the transmission power of the nodes according to (15) and later to perform decision fusion according to (6).

For decision combining all nodes have to transmit their local decisions u_j over the wireless channel to the fusion center. Since we process the stored data off-line, we artificially introduce these communication channels by simulations to validate the power assignment strategy from Section III. In the simulation we consider path loss according to $d_j^{-\beta}$, with d_j denoting the distance from S_j to the fusion center. The considered simulation parameters are given in Table I.

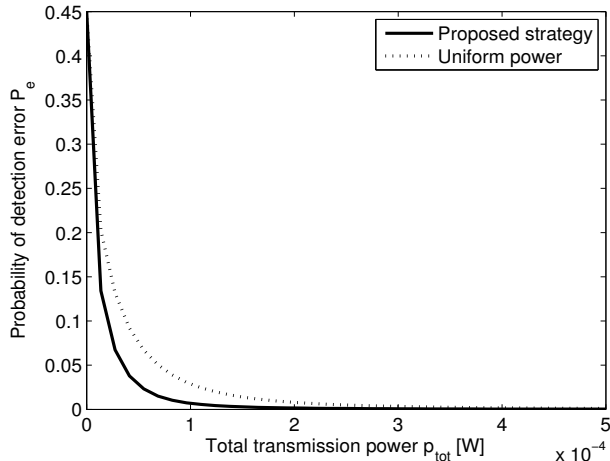


Fig. 6. Probability of detection error P_e depending on the total transmission power p_{tot} for the proposed strategy and uniform power assignment.

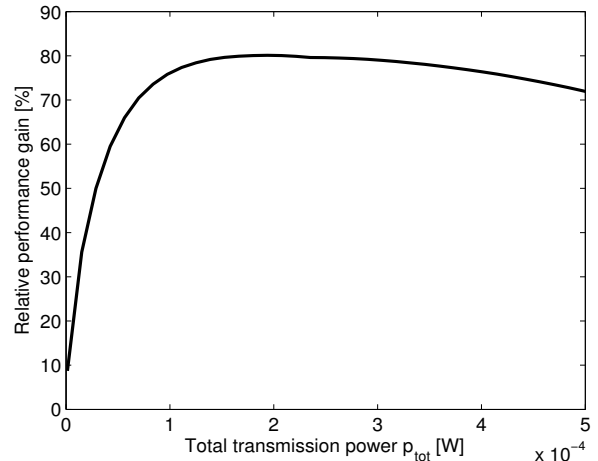


Fig. 7. Relative performance gain of the proposed strategy in terms of the reduction of the global probability of detection error P_e compared to uniform power assignment.

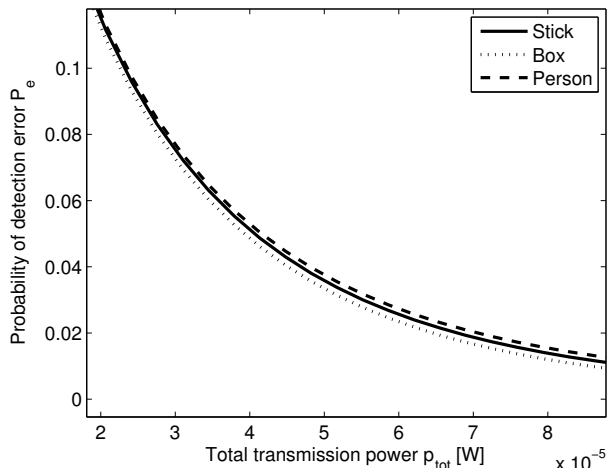


Fig. 5. Probability of detection error P_e depending on the total transmission power p_{tot} for different target objects.

VI. NUMERICAL RESULTS

In this section, we analyze the performance of the distributed target detection system in terms of the global probability of detection error P_e at the fusion center.

Fig. 5 shows the global probability of detection error P_e depending on the total transmission power p_{tot} for the three

TABLE I
PARAMETERS USED IN THE SIMULATION

parameter	value
β	2
σ^2	$1.9966 \cdot 10^{-3}$
N_j	10
T_f	100 ns
η	10^{-11} J

different target objects and uniform power allocation, i.e., all nodes transmit with the same power. With increasing p_{tot} , P_e decreases since the bit-error probability of the channel (4) is lowered. The system shows almost the same detection performance for the three target objects. Yet, the metal objects (stick and box) are slightly easier to detect than a person. Due to the similar behavior we focus on the results of the metal stick to evaluate the influence of the application-specific power assignment strategy. The results are given in Fig. 6 and Fig. 7. Fig. 6 shows P_e depending on p_{tot} for the proposed strategy and uniform power allocation. It can be observed that the proposed strategy results in a lower P_e over the entire range of the analyzed transmission power. Fig. 7 states that a significant relative performance gain in terms of a reduction of the global probability of detection error P_e can be achieved by using the proposed power assignment strategy.

VII. CONCLUSIONS

In this paper, we have analyzed the performance of a distributed target detection system for wireless sensor networks, which utilizes ultra-wideband technology both, for the sensing and the communication task. Depending on the individual detection performance of the nodes, we have proposed a cross-layer approach for assigning transmission power to the communication task, with the goal to optimally distribute a total budget of transmission power, with respect to the global probability of detection error. It has been evaluated by a hybrid approach consisting of real UWB-radar measurement data and simulations results. It leads to significant performance gains compared to uniform power allocation.

In future work the presented approach might be extended to a joint optimization of the transmission power for the radar and the communication task.

ACKNOWLEDGMENT

This work was supported by the Deutsche Forschungsgemeinschaft (DFG) project UKoLoS and the UMIC excellence cluster of RWTH Aachen University.

REFERENCES

- [1] L. Dan, K. Wong, Y. H. Hu, and A. Sayeed, "Detection, classification, and tracking of targets," *IEEE Signal Process. Mag.*, vol. 19, no. 2, pp. 17–29, Mar. 2002.
- [2] J.-F. Chamberland and V. Veeravalli, "Wireless sensors in distributed detection applications," *IEEE Signal Process. Mag.*, vol. 24, no. 3, pp. 16–25, May 2007.
- [3] B. Chen, L. Tong, and P. Varshney, "Channel-aware distributed detection in wireless sensor networks," *IEEE Signal Process. Mag.*, vol. 23, no. 4, pp. 16–26, 2006.
- [4] R. Srinivasan, "Distributed radar detection theory," *IEE Proceedings-F*, vol. 133, no. 1, pp. 55–60, Feb. 1986.
- [5] L. Pescosolido, S. Barbarossa, and G. Scutari, "Radar sensor networks with distributed detection capabilities," in *Proc. IEEE Int. Radar Conf.*, 2008, pp. 1–6.
- [6] J. Sachs, P. Peyerl, and M. Rossberg, "A new UWB-principle for sensor-array application," in *Proc. IEEE Instrument. and Measur. Techn. Conf. IMTC/99*, vol. 3, 1999, pp. 1390–1395.
- [7] M. Win and R. Scholtz, "Ultra-wide bandwidth time-hopping spread-spectrum impulse radio for wireless multiple-access communications," *IEEE Trans. Commun.*, vol. 48, no. 4, pp. 679–689, Apr. 2000.
- [8] D. Warren and P. Willett, "Optimum quantization for detector fusion: some proofs, examples, and pathology," *J. Franklin Inst.*, vol. 336, pp. 323–359, 1999.
- [9] D. Bielefeld and R. Mathar, "Topology generation and power assignment in IR-UWB networks," in *Proc. IEEE Int. Symp. Wireless Commun. Syst. (ISWCS)*, Oct. 2007, pp. 277–281.
- [10] D. Bielefeld, G. Fabek, and R. Mathar, "Power-aware distributed detection in IR-UWB sensor networks," in *Proc. IEEE Sensor Array and Multich. Signal Process. Workshop (SAM)*, Jul. 2008, pp. 261–265.
- [11] J. Fiorina and W. Hachem, "On the asymptotic distribution of the correlation receiver output for time-hopped uwb signals," *IEEE Trans. Signal Process.*, vol. 54, no. 7, pp. 2529–2545, 2006.
- [12] A. W. Bowman and A. Azzalini, *Applied smoothing techniques for data analysis: the kernel approach with S-Plus Illustrations*. Oxford University Press, 2004.